24th International Conference on Renewable Energies and Power Quality (ICREPQ'26)
Santander (Spain), 10th to 12th June 2026
ISBN-13: 978-84-09-82044-3

# Influence of the Gap Distance on the Repetition Rate and Apparent Discharge Power in Corona Discharges

M. Soltany[1], J.-R. Riba[1], P. Canalda[1] and S. Bogarra[1]

[1] Department of Electrical Engineering
AMBER High-Voltage Laboratory, Universitat Politècnica de Catalunya
Campus of Terrassa – 0822 Terrassa (Spain). +34 937398365, jordi.riba-ruiz@upc.edu

**Abstract.** Testing for corona discharges is a major step in design and development of high-voltage equipment. Apparent discharge power is considered an important indicator of insulation stress, as it relates to discharge magnitude and pulse repetition rate. This study investigates the effect of gap distance, applied voltage and electrode geometry on apparent discharge power, based on the principles of IEC 60270. Partial discharge (corona) measurements were performed under controlled laboratory conditions and at a fixed pressure, using two common configurations: rod-plane and sphere-plane. The gap distance between the test object and the ground plane was varied, and voltages corresponding to 110% and 120% of corona inception voltage (CIV) were applied. The results presented in this work demonstrate that apparent discharge power decreases significantly with an increase in the gap distance, with the most dramatic change occurring at small gaps. Furthermore, the impact of electrode geometry on apparent discharge power is analyzed, with spherical electrodes producing significantly higher levels than rod electrodes under identical voltage conditions.

**Key words.** Corona discharges, apparent discharge power, apparent charge, discharge repetition rate.

## 1. Introduction

Partial discharges are an unavoidable part of any power system installation operating at high voltage. They are defined as localized electrical discharges that only partially bridge the insulation between the high voltage and the ground electrodes [1]. Partial discharges can occur in the vicinity of a conductor (corona discharges), on the surface of an insulating material (surface discharges) or within the bulk of the insulation (internal discharges).

Corona is a type of partial discharge that occurs due to a high degree of electric field non-uniformity in the gaseous medium surrounding a conductor [2], [3]. Despite growing interest in using the corona phenomenon in processes such as chemical extraction [4], water treatment, and industrial applications, corona can seriously damage insulation in power systems and cause notable energy losses.

There is an ongoing rapid evolution of electrical power systems, in which electric vehicles, high-speed trains, and modern power electronic devices are increasingly being integrated. These developments have raised the demand for electrical energy. Consequently, power lines are being operated closer to their maximum limits, which increases the probability of corona occurrence. On the other hand, special care must be taken during the manufacturing of new power equipment to avoid partial discharge activity.

In studies related to partial discharges, particularly corona discharges, the activity is usually assessed by measuring the apparent charge, pulse repetition rate, pulse duration and temporal characteristics of the pulses (e.g., timing within the AC cycle or intervals between consecutive pulses in AC and DC). Other studies focus on the behavior of partial discharges, such as defect localization using the visible and ultraviolet light emission during the ionization process [5], or acoustic signals under various conditions or applied voltages. While these studies provide valuable information on pulse detection, characterization and localization, they do not quantify the power associated with the discharges.

The apparent discharge power is a parameter introduced to quantify the power associated with ionization, and it is already defined in the IEC 60270 standard [1]. While it is well known that the behavior of partial discharge pulses varies with different configurations and conditions, the variation of apparent discharge power for different geometries and gap distances, especially under corona activity, is still not fully understood.

This study focuses on an experimental investigation of the apparent discharge power of corona at atmospheric pressure using two electrode geometries. By analyzing the effects of gap distance and applied voltage, the study aims to clarify the influence of geometry on discharge power for insulation condition assessment.

The study is structured as follows. Section 2 describes the concepts and formulations of apparent charge and discharge power. Section 3 presents the experimental setup used to generate and measure PD pulses. Section 4 explains the methodology used to measure PD parameters in all cases. Section 5 summarizes and discusses the results obtained. Section 6 presents the conclusions.

## 2. Apparent charge and apparent discharge power according to IEC 60270

The electric charge involved in the discharge activities cannot be measured directly due to limitations in accessing the discharge terminals and the transient, high-speed nature of discharge events [6]. For this reason, the IEC 60270 standard proposes the concept of apparent charge, which is the charge that would result in the same reading on the measuring instrument as the PD pulse itself if injected between the terminals of the test object in a specified test circuit [1].

Assuming a linear measuring impedance with transfer impedance $Z_m$, the numerical integration of the PD pulse current over time can be used to calculate the apparent charge:

$$q_{pulse} = \int_{t_1}^{t_2} i(t)dt = \int_{t_1}^{t_2} [u(t)/Z_m]dt \quad (1)$$

where $u(t)$ is the voltage measured by the PD instrument, $Z_m$ is the corresponding transfer impedance and $t_2 - t_1$ is the duration of the PD pulse.

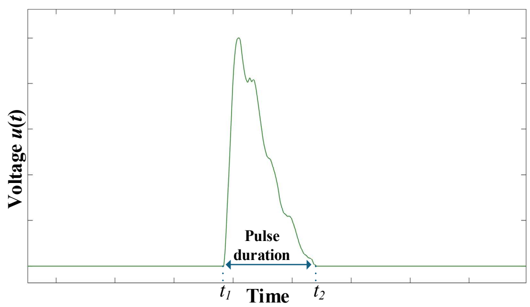

Figure 1. Apparent charge calculation from PD pulse.

Apparent discharge power, $P$, is a derived quantity that consists of the average pulse power fed into the terminals of the test object due to the apparent charge magnitudes $q_i$ during a chosen reference time interval $T_{ref}$ [1],

$$P = \frac{1}{T_{ref}}(q_1u_1 + q_2u_2 + ... + q_iu_i) \quad (2)$$

where $u_1$, $u_2$, ..., $u_i$ are the instantaneous values of the test voltage at the times of occurrence, $t_i$, of the individual apparent charge magnitudes, $q_i$.

## 3. Experimental setup

In this study, in order to obtain the PD pulses, a standard measurement circuit according to IEC 60270 is used, which can be seen in Figure 2.

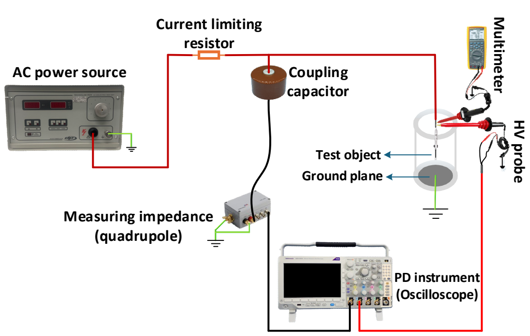

Figure 2. Schematic of the experimental setup.

An adjustable AC power source with nominal ratings of 0–14 kV-peak, 600 VA and 50 Hz was used to adjust the high voltage at the terminals of the test object. Two high-voltage probes (Testec HVP-40, 0–300 Hz, 28 kV RMS AC voltage, 1:1000 division ratio) were used simultaneously. One probe was connected to a true RMS multimeter (Fluke 289, accuracy ≥ 0.4%, frequency range 5–100 kHz) to measure the sinusoidal voltage applied to the test object. The other probe was connected to one channel of an oscilloscope (Tektronix MDO324, sampling rate 2.5 GS/s, 11-bit vertical resolution) to observe the instantaneous sinusoidal waveform, which was then used to calculate the apparent discharge power. The oscilloscope was also used as a PD instrument to acquire the PD pulse voltage waveforms measured at the output of the quadrupole. With a bandwidth of 200 MHz, the oscilloscope aligns with the IEC 60270 requirement (≥ 50 MHz) for apparent charge calculation by numerical integration. Using the oscilloscope offers practical advantages, including lower cost compared to specialized devices such as PDbase, and the ability to analyze the parameters associated with the partial discharge pulses including amplitude, duration, rise time and fall time.

In parallel with the test object, the measurement branch consisted of a coupling capacitor (TDK FHV-6AN, 3500 pF, 30 kV-peak) and a quadrupole (Omicron CPL452, 20 kHz–6 MHz).

To verify the consistency of the results, two geometries of different shapes that are commonly used were employed: a stainless steel sphere with a diameter of 3 mm and a stainless steel rod with a diameter of 1.2 mm. Figure 3 shows the sphere and rod electrodes in detail.

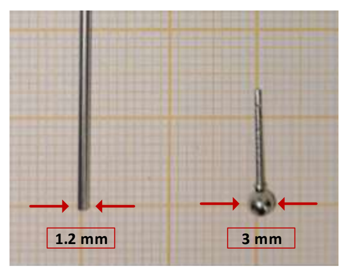

Figure 3. Details of the geometries used in the experiments.

## 4. Methodology

During the experiments, the vertical distance between the test object and the horizontal ground plane was changed. The following gap distances were considered: 10 mm, 20 mm, 40 mm, 70 mm and 100 mm. At each distance, the voltage was slowly increased to determine the corona inception voltage (CIV), at which point only one single discharge pulse is triggered on the oscilloscope in each sinusoidal cycle. Then, the voltage was increased gradually to 1.1×CIV and 1.2×CIV, with five samples acquired at each voltage level for averaging purposes. All tests were conducted at a pressure of 100 kPa and temperature of between 21°C and 23°C.

The files recorded from the oscilloscope contained both the sinusoidal supply waveform and the PD pulses. In the next step, a MATLAB® code was used to calculate the relative apparent discharge power according to (2). The code also counted the PD pulses in each cycle to assess the effects of distance and geometry on the repetition rate.

Figure 4 shows two oscilloscope acquisitions for both geometries.

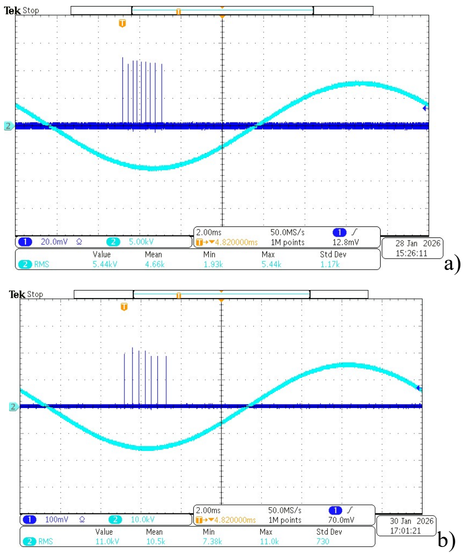

Figure 4. Oscilloscope acquisitions at 100 kPa and a 40 mm distance. a) 1.2 mm rod at 1.1CIV = 5.44 kV-RMS. b) 3 mm sphere at 1.1CIV = 11.0 kV-RMS.

## 5. Results

For a constant pressure and distance, the PD pulse repetition rate depends on the geometry, as shown in Figure 4. This is further illustrated by the results in Table I, which reports the repetition rate of the rod and sphere electrodes at different distances and voltage levels. The repetition rates are given as the average of five oscilloscope acquisitions, plus or minus the standard deviation.

Table I. PD pulse repetition rates at 100 kPa for two electrode geometries.

| Distance (mm) | Voltage | Repetition rate (pulses per cycle) | |
|---|---|---|---|
| | | Rod | Sphere |
| 10 | 1.1 CIV | 42.4 ± 2.7 | 27.6 ± 2.7 |
| | 1.2 CIV | 104.0 ± 1.4 | 93.0 ± 2.2 |
| 20 | 1.1 CIV | 15.4 ± 1.3 | 11.0 ± 0.0 |
| | 1.2 CIV | 40.2 ± 1.7 | 34.6 ± 4.0 |
| 40 | 1.1 CIV | 9.0 ± 0.0 | 6.4 ± 0.5 |
| | 1.2 CIV | 21.8 ± 0.4 | 15.6 ± 0.5 |
| 70 | 1.1 CIV | 8.2 ± 0.4 | 6.0 ± 0 |
| | 1.2 CIV | 19.0 ± 0.0 | 14.0 ± 0.0 |
| 100 | 1.1 CIV | 8.0 ± 0.0 | 6.0 ± 0.0 |
| | 1.2 CIV | 16.8 ± 0.4 | 12.4 ± 0.5 |

As shown in Table I, for a fixed gap distance, the pulse repetition rate of the rod is higher than that of the sphere at both voltage levels. This is because the sharper and smaller geometry of the rod produces a more non-uniform electric field, with higher field intensity at the tip, leading to increased ionization activity in that region. Moreover, for both geometries, the repetition rate increases with decreasing distances, but the trend is not uniform; for the smaller distances (≤ 20 mm), the repetition rate increases faster.

Figure 5 provides a clearer visual representation of the average values of the repetition rate reported in Table I.

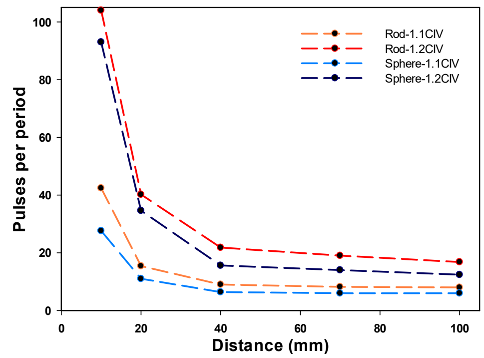


Figure 5. Changes in the repetition rate (pulses per second) for the two geometries at different distances and 100 kPa.

According to the results presented in Figure 5, in the event of insulation ageing and degradation, smaller, sharper defects are more critical, as they produce more partial discharge (PD) pulses per second. However, another important observation from Figure 4 is that, for a larger object (the sphere), the PD pulse amplitude is almost four times greater than that of the rod. This demonstrates that pulse repetition rate alone cannot be used to evaluate the damage caused by partial discharges. Hence, the apparent discharge power provides a more comprehensive measure of the severity of PD activity, as it takes into account the number of pulses within a given period, the apparent charge magnitude of each pulse, and the corresponding instantaneous voltage.

Table II presents the apparent discharge power calculated from (2) for both geometries at the different analyzed distances. As with the repetition rate, the values are given as the average of five measurements, together with the corresponding standard deviation.

Table II. Apparent discharge power at 100 kPa for two geometries.

| Distance (mm) | Voltage | Apparent discharge power (µW) | |
|---|---|---|---|
| | | Rod | Sphere |
| 10 | 1.1 CIV | 2331 ± 33 | 11177 ± 619 |
| | 1.2 CIV | 6354 ± 72 | 34835 ± 874 |
| 20 | 1.1 CIV | 722 ± 69 | 4917 ± 149 |
| | 1.2 CIV | 2070 ± 51 | 13701 ± 349 |
| 40 | 1.1 CIV | 376 ± 11 | 2568 ± 166 |
| | 1.2 CIV | 977 ± 25 | 6374 ± 195 |
| 70 | 1.1 CIV | 364 ± 5 | 2298 ± 29 |
| | 1.2 CIV | 835 ± 23 | 4947 ± 99 |
| 100 | 1.1 CIV | 348 ± 31 | 2108 ± 156 |
| | 1.2 CIV | 776 ± 37 | 4711 ± 22 |

According to Table II, in contrast to the repetition rate, the apparent discharge power is much higher for the sphere in all cases. This can be justified by the effects of capacitance and applied voltage. According to [6] and [7], the apparent charge depends on the capacitance of the configuration. As the size of the object increases, the capacitance also increases. Consequently, a larger test object tends to exhibit higher discharge pulse amplitudes. Additionally, as the object size increases, a higher voltage is required to initiate ionization activity in the surrounding air insulation medium. For instance, at a distance of 40 mm, the CIV for the sphere was 10 kV, while for the rod it was 4.94 kV. This higher voltage level leads to a larger apparent charge magnitude and, therefore, higher apparent discharge power.

As for the repetition rate, the apparent discharge power increases significantly as the distance decreases, indicating that defects with shorter gap distances in actual high-voltage equipment can degrade much faster in the event of discharge activity.

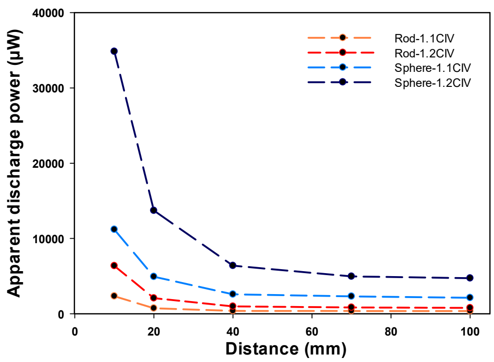


Figure 6. Variation of the apparent discharge power for the two geometries at different distances and 100 kPa.

According to Figure 6, the difference in discharge power between the sphere and the rod is so significant that, for a fixed distance, not only is the power higher at the same relative voltage, but the power at 1.1 CIV for the sphere even exceeds that at 1.2 CIV for the rod.

## 6. Conclusion

Corona discharges can damage electrical system insulation and lead to noticeable power losses. This study investigated the partial discharge repetition rate and apparent discharge power for different gap distances and voltage levels. Two configurations, comprising a 3 mm diameter sphere and a 1.2 mm diameter rod, were tested at atmospheric pressure. The results can be summarized as follows:

1- For smaller and sharper test objects, the repetition rate is higher due to the strong concentration of the electric field near the tip and sharp edges.
2- The repetition rate alone is not a reliable parameter for evaluating discharge harmfulness, since it does not consider the discharge magnitude or the applied instantaneous voltage. This can be directly related to the actual defects present in high voltage equipment. For example, sharp defects such as needle-like protrusions in conductors or connectors tend to produce high repetition rates but relatively lower discharge power, whereas larger defects or contaminants may generate fewer but more energetic discharges.
3- Apparent discharge power can be used to evaluate the severity of discharges or to compare different defects in high voltage equipment and insulation design.
4- By decreasing the gap distance, both the repetition rate and the apparent discharge power increase. This increase is much more pronounced at shorter distances, but it also depends on the configuration and geometry. For the test objects analyzed in this study, at distances below 40 mm, a significant increase was observed. This indicates that insulation systems with reduced clearances are more vulnerable to degradation under corona activity.

Although apparent discharge power is a well-known parameter in the literature, this study shows its sensitivity to electrode geometry and gap distance under corona conditions. This provides valuable insights for practical partial discharge measurements.

## Acknowledgement

This project received funding from grant PID2023-147016OB-I00 by MICIU/AEI/10.13039/501100011033/ and by ERDF "A way of making Europe," by the European Union and from the Agència de Gestió d'Ajuts Universitaris i de Recerca-AGAUR (2021 SGR 00392).

## References


[1] IEC, IEC 60270: 2025 High-voltage test techniques - Charge-based measurement of partial discharges. Geneve, Switzerland: International Electrotechnical Commission, 2025.

[2] J.-R. Riba, "Linking digital image intensity to carrier density in low-pressure corona discharges," *Sensors Actuators A Phys.*, vol. 359, p. 114474, 2023.

[3] J.-R. Riba, C. Abomailek, P. Casals-Torrens, and F. Capelli, "Simplification and cost reduction of visual corona tests," *IET Gener. Transm. Distrib.*, vol. 12, no. 4, pp. 834–841, Feb. 2018.

[4] S. Machmudah *et al.*, "Phytochemical compounds extraction from medicinal plants by subcritical water and its encapsulation via electrospraying," *Alexandria Eng. J.*, vol. 61, no. 3, pp. 2116–2128, Mar. 2022.

[5] M. Soltany, J.-R. Riba, and S. Bogarra, "On the scaling of digital cameras to quantify the intensity of corona discharges," *Measurement*, vol. 265, p. 120343, Mar. 2026.

[6] Eberhard Lemke *et al.*, "Guide for electrical Partial Discharge Measurements in compliance to IEC 60270," *Electra*, vol. 241, no. Technical Brochure 366, pp. 61–67, 2008.

[7] R. Haller, J. Hornak, P. Martinek, and J. Hlavacek, "Simple Calibration Method for Improving the Comparability of PD Measurement Results at HVDC Conditions," *Lect. Notes Electr. Eng.*, vol. 599 LNEE, pp. 1249–1256, 2020.